Mitochondrial Communications 3 (2025) 66–78

Contents lists available at ScienceDirect

Mitochondrial Communications

journal homepage: www.keaipublishing.com/en/journals/mitochondrial-communications

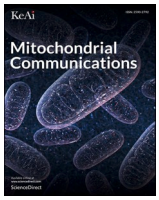

Research Article

Age-related dynamics of m.189A>G and m.408T>A variants in skeletal muscle of an osteoarthritic Cohort: Connections to BMI and muscle strength

Valeria Lobanova [a,*,e], Ivan Kozenkov [a,e], Eldar Khaibulin [a,e], Maria Tatarkina [a,e], Bogdan Efimenko [a], Viktoria Skripskaya [a], Akhsarbek H. Dzhigkaev [a,b], Anastasia S. Krylova [a], Anastasia V. Prokopenko [c], Stepan V. Toshchakov [c], Andrey Goncharov [a,f], Konstantin Popadin [a,f], Konstantin V. Gunbin [a,d,f]

[a] Immanuel Kant Baltic Federal University, Kaliningrad, Russia
[b] Federal State Budgetary Institution "Federal Center for High Medical Technologies" of the Ministry of Health of the Russian Federation, Kaliningrad, Russia
[c] National Research Center "Kurchatov Institute", Moscow, Russia
[d] Institute of Molecular and Cellular Biology SB RAS, Novosibirsk, Russia

ARTICLE INFO

Keywords:
Mitochondrial DNA
SNP
Osteoarthritis
Aging

ABSTRACT

The origin and expansion of mitochondrial somatic variants, influenced by tissue-specific mutagenesis and selection, are not well understood despite their relevance to aging and age-related diseases. Postmitotic tissues, such as skeletal muscles, are particularly underexplored, even though mtDNA variant evolution in these tissues can differ significantly from that in proliferative tissues. To address this, we analyzed mitochondrial heteroplasmy in skeletal muscle samples from an osteoarthritic cohort (N = 105). We observed that the age-related dynamics of two famous variants m.189A > G and m.408T > A in our cohort is indistinguishable from their dynamics in random control cohort, suggesting that they are not a cause of muscular problems, but rather mark the age-related processes in muscles. We also observed that when adjusted by age and gender, carriers of these variants tend to have higher BMI, body weight, and muscle strength than non-carriers. Putting together all the lines of evidence, we propose that these variants are able to rapidly expand through selfish dynamics, which is especially pronounced in hypertrophic muscle fibers of individuals with higher body weight. Further investigation is necessary to clarify this hypothesis.

1. Introduction

The accumulation of mutations in the mitochondrial genome can strongly affect mitochondrial functionality. The phenotypic manifestation of mutations depends on the amount of mutant mtDNA present in mitochondria, which is known as the threshold of heteroplasmy. Some in vitro studies have shown that the proportion of mtDNA mutations leading to phenotypic manifestation is approximately 90 %.[1,2] It has also been observed that heteroplasmic variants are more common in some positions, especially in the control region (CR),[3,4] which suggests that these variants have a specific impact on the stability of mtDNA and may influence the control of mitochondrial transcription and replication through potential changes in secondary mtDNA structure.[5]

Various mtDNA lesions, including insertions, deletions, duplications, and point mutations, can be caused by increased oxidative stress, which occurs in tissues with higher metabolism, especially in postmitotic tissues.[6] Moreover, it is assumed that rapidly dividing cells have more effective selection against heteroplasmy while postmitotic cells, such as muscle cells and neurons, accumulate mutations due to reduced selection pressure against cells with mitochondrial dysfunction.

Harman,[7] followed by Beckman and Ames,[8] presented and provided compelling arguments about the free radical theory of aging, which states that free radical production grows with age and plays an essential role in senescence processes. Several papers have demonstrated

Peer review under the responsibility of Editorial Board of Mitochondrial Communications.
* Corresponding author. Universitetskaya st., 2, 236006, Kaliningrad, Russia.
E-mail address: valeriavlobanova@gmail.com (V. Lobanova).
[e] Coequal first.
[f] Coequal last.

https://doi.org/10.1016/j.mitoco.2025.08.001
Received 21 November 2024; Received in revised form 1 June 2025; Accepted 3 August 2025
Available online 5 August 2025

increased mtDNA damage associated with the healthy aging of skeletal muscle. Point mutations in the mitochondrial genome begin to accumulate in muscle tissues with age, as evidenced by the screening of individuals aged over 20.[9] Moreover, among individuals over the age of 70, along with muscular heteroplasmic mutation accumulation, approximately 50 % have at least one mtDNA duplication in both muscle and bone tissues.[10] Thus, in our study of patients experiencing a combination of healthy and pathologic aging due to osteoarthritis, we decided to focus on the accumulation of mtDNA mutations in human muscle tissue. The aging and unhealthy body weight are largely responsible for osteoarthritis,[11] for which joint pain and stiffness are the most common symptoms, which can lead to decreased functionality, loss of activity, low quality of life, and regular usage of various nonsteroidal anti-inflammatory drugs (NSAIDs). The knee and hip joints are most commonly affected by osteoarthritis; therefore, we used samples from the skeletal muscles immediately adjacent to these joints. The use of skeletal muscle samples from this problematic region allowed us to perform complex analyses of both healthy and pathologic aging.

Based on next-generation sequencing (NGS) analysis of skeletal muscles, we found several somatic single-nucleotide polymorphisms (SNPs) in heteroplasmy, two of which — m.189A > G and m.408T > A — had extremely high frequencies in our osteoarthritic cohort. These mitochondrial variants have previously been observed in muscle (skeletal muscle and myocytes); the former has also been observed in bone tissues[12] and is associated with aging.[10] For example, approximately 20 % of people aged over 60 have the m.189A > G SNP, and its level of heteroplasmy in muscle tissue is easily detectable and increases with age.[13,14] We propose that the patients in our osteoarthritic cohort may have had dystrophic muscle changes; however, those with the m.189A > G and m.408T > A SNPs may have experienced a compensatory effect, especially in muscle function, as evidenced by higher dynamometry results.

MtDNA mutations connected with diseases often result in tissue-specific heteroplasmic patterns, which are believed to be the result of tissue-specific positive selection for the different bioenergetic demands of different tissues.[5] It would be intriguing to determine whether the mtDNA copy number is connected to mtDNA heteroplasmy. To answer this, we linked the molecular details of observed m.189A > G and m.408T > A SNPs to the clinical data of a given cohort by taking into account both structural and functional data regarding the location of mutated positions. Human mtDNA has a very close relationship between the m.189A > G transition and the primary site of H-strand DNA synthesis initiation — that is, position 191 (OH1[15,16]). The m.408T > A transition occurs beyond the midpoint of the mtDNA L-strand transcription promoter, which is located at position 407 (LSP[15,16]). Indeed, our study reveals that the molecular effects of the m.189A > G and m.408T > A SNPs are connected to mtDNA replication and transcription, which are involved in shaping mtDNA copy numbers, although we cannot dismiss a potential link between mtDNA copy number changes and patient health status.

2. Materials and methods

2.1. Patient physiology

All volunteers were measured for height, weight, muscle strength, and blood pressure. Before surgery, their biochemical and general blood test results were evaluated. Leukocyte indices were also calculated for all patients.

2.2. Biosamples and sample preparation

The materials used in this study were biopsy specimens of muscle tissue and adjacent connective and adipose tissues with a volume of 10–50 cubic millimeters, obtained during knee or hip joint endoprosthesis surgery. Obtaining such volumes of biopsy specimens is safe, does not harm the patient's health, and does not affect their recovery process. Immediately after excision, the samples were placed in 15 ml of isotonic solution with a mixture of antibiotics to prevent bacterial contamination. The biopsy material was obtained from August 2021 to December 2022 at the Department of Traumatology and Orthopedics of the Federal Center for High Medical Technologies, the Federal State Budgetary Institution of the Ministry of Health of the Russian Federation, in Rodniki Village in Kaliningrad, Russia. Before their operations, all volunteers provided informed consent to participate in the research, which was conducted in strict compliance with the World Medical Association's Declaration of Helsinki and the International Council for Harmonisation's Guideline for Good Clinical Practice. This study was approved by the independent ethical committee of Immanuel Kant Baltic Federal University and by the ethical committee of the Federal Service for Surveillance in Healthcare.

2.3. Mitochondrial DNA isolation and purification

To determine mtDNA heteroplasmy and detect de novo mutations, special methods were required for the isolation, enrichment, and purification of mtDNA at the essential quantity (up to 500 ng) to prepare PCR-free NGS libraries. For this, we decided to use an approach similar to that used in Ref. 17 with a protocol based on.[18]

The isolation and purification of mtDNA were performed the day after obtaining the biopsy materials at the Center for Genomic Research of Immanuel Kant Baltic Federal University. In postmitotic tissue cells, the mitochondrial genome accounts for up to 1 % of total DNA. By conducting tuning experiments (i.e., selecting the optimal proteolytic and nuclease ferments and cleaning the final fraction of mtDNA from the ferments) with various parameters (time of primary proteolysis, initial volume and quality of tissue, and setting up stages of nuclease activity), we adapted methods for the enrichment of mitochondrial fractions and the purification of mtDNA. We proceeded on the basis of a well-developed intercellular matrix (collagen, fibrin, and elastin), which needed to be discarded so that work could be conducted with individual muscle fibers in the homogenisation process. Because of this, we tested various proteinases (proteinase K, trypsin, and collagenase) and compared their efficiency.

Tissues were treated with collagenase from crab pancreas and homogenized using a Dounce homogenizer. Mitochondria were then isolated, and nuclear DNA and RNA were removed using plasmid-safe ATP-dependent DNase I (Lucigen) to preserve mitochondrial circular DNA and RNase A. Mitochondrial membranes were dissolved with a composition of proteinase K, RNase A, and lysis buffer. Mitochondrial DNA was extracted using the phenol–chloroform method, and additional purification of nonring DNA fragments was also performed. For this, we again used proteinase K, DNase I, and RNase A to remove the histone complexes linked to gDNA and then cleavaged the gDNA and RNA leftovers.

The degree of purity of mtDNA from the impurities was assessed using PCR screening for the beta-actin gene region and Alu repeats (AluSx) (see the sequences in Supplementary Text S3) in the human genome (DNA from HEK-293 cells). Housekeeping genes, such as 18S (18S rRNA), GAPDH, HPRT1, YWHAZ, UBC, RPII, and POLR2A (RNA polymerase II), are usually used for such analyses. However, these genes are single-copy; that is, they occur only once in the gDNA. In our work, we decided to use Alu repeats — that is, short dispersed nuclear elements (SINEs) 100–900 bp in length, specific to primates — as the target site. The human genome consists of approximately 10 % Alu repeats,[19] which are fairly evenly distributed throughout chromosomes. In primate genomes, there are more than 1 million copies of Alu repeats.[20] This is why such repeats are more reliable markers for the detection of gDNA by PCR than housekeeping genes. In this study, we focused on the AluSx repeat family and selected primers for the repeats' 5B and 3B shoulder regions to amplify fragments from 200 to 600 bp.

To normalize the amount of genomic material, a method for quantitatively assessing mtDNA copy numbers was developed.

2.4. DNA copy number identification

The relative mtDNA copy numbers of the samples were measured using real-time PCR with SYBR Green I intercalating dye (qPCRmix-HS SYBR-low ROX kit (Eurogen, Moscow, Russia)). As an internal control sample, we used mtDNA no. 62 rasterized to concentrations of 10 ng/μL, 1 ng/μL, and 0.1 ng/μL. For all PCR variants, we used the same primer pairs for the ND5, CYTb, act-b, and AluSx gene regions. The primer sequences and the lengths of the expected amplification products are provided in Supplementary Text S4. The melting curves of amplification products for real-time PCR, as well as tabular data, are available from the link in Supplementary Text S5.

The copy numbers of the mtDNA molecules were calculated by the NEB web calculator using the following formula:

$$\text{dsDNA [mol]} = \text{dsDNA mass [g]} / ((\text{dsDNA length [bp]} * 617.96\ [\text{g/mol}] / [\text{bp}]) + 36.04\ [\text{g/mol}])$$

$$\text{DNA copy number} = \text{dsDNA [mol]} * 6.022 * 1023.$$

Considering the length of mtDNA to be 16,569 bp, using the above formulas we obtained a value equal to 58.82 million copies of mtDNA molecules in 1 ng.

2.5. DNA sequencing

Library preparation and NGS sequencing were performed at the Kurchatov Genomic Center at the Kurchatov Institute. The libraries of 101 samples were prepared on the basis of HyperPlus Kit PCR-free #07962410001 (Roche) KAPA, while 48 samples were processed using the PCR-free method. Sequencing was performed using Illumina NovaSeq (48 samples) and Illumina MiSeq (57 samples) platforms. Another eight samples were sequenced using the MGISeq DNBSEQ-G400 platform, and libraries were prepared using the MGIEasy Universal DNA Library Prep Set.

For 31 samples, the coverage was over 100 × . The coverage of the mitochondrial genome ranged from 9 × to 1756 × . The number of mapped reads ranged from 2 % to 48 %.

2.6. Variant calling pipeline

The variant calling pipeline consisted of two steps: (1) preparation of raw FASTQ data and reads pre-alignment on the GRCh38 human genome and (2) refinement of the alignment of probable mtDNA reads, followed by mitochondrial SNP/MNP (multiple nucleotide polymorphism) calling and final filtration (for details, see Supplementary Text S6). For the first step, we used BBMAP v. 39.00 software[21] to perform various read filtering procedures and BWA mem v. 0.7.17-r1188 software[22] to pre-align reads onto the reference genome. In the second step, mtDNA SNP/MNP variants were called using sophisticated MitoHPC v. 20240109[23] software, which takes into account patient-specific mtDNA consensus. To completely eliminate any potential NUMT variants, we filtered the variants based on (1) the quality of reads containing SNPs/MNPs using bam-readcount v.1.0.1.[24] and (2) the appearance of SNPs/MNPs in previously available population data using the gnomAD v3.1[25] and HelixMTdb_20200327[26] databases. In this second step, we also separated the mtDNA variants into two groups (for details, see Supplementary Text S6): stringent (variants that met the most stringent filtering criteria) and relaxed (both stringent variants and variants with some bias in variant-calling statistics, which are not essential to accurately identify true mtDNA variants).

2.7. Age–VAF correlation and comparison with Li et al.'s (2015) cohort

To investigate the correlation between age and variant allele frequency (VAF) in the osteoarthritic cohort, we performed a linear regression analysis using the linregress function from the scipy.stats library.[27] This analysis was conducted for both strictly and loosely filtered variants data.

We then expanded our analysis to compare our findings with data from the Li et al. (2015) cohort. We filtered data from Ref. 5 to include either the m.189A > G or m.408T > A variants identified in skeletal muscle, thereby ensuring consistency with our patient data. We then assessed whether the age–VAF correlation observed in our patient group aligned with that in the Li et al. (2015) cohort. Specifically, we checked whether the VAF values in our patients fell within the confidence interval of the linear regression model derived from the Li et al. (2015) control group.

2.8. Fisher's exact test

Fisher's exact test was conducted to assess the distribution of VAF across different age ranges. The patients were categorized into age groups, from which we counted the number of patients whose VAF was higher or lower than the predicted value from the linear regressions for their ages. The test used a contingency table in the following form:

$$[[A, B], [C, D]]$$

where A represents the number of patients within an age range with a VAF higher than predicted, B represents those with a lower VAF, and C and D represent the corresponding counts for the Li et al. (2015) cohort. The fisher_exact function from the scipy.stats library was used for this analysis.

2.9. Randomization of sums

To compare the mtDNA variants (here and below, we consider the variants detected by the stringent filter) between our five patient groups and the overall patient population, we employed a randomization approach. We generated 10,000 random samples with replacements from the entire patient population, with each sample size matching the size of the specific patient group being compared. We then compared the sum of the feature values for each patient group with the sum for each random sample, counting the number of instances in which the group's sum was greater. This process was repeated for every clinical feature collected (the function code is available from the link in Supplementary Text S1).

2.10. Primary vs. posttraumatic arthritis comparison

A comparison between patients with primary and posttraumatic arthritis was performed using bootstrap sampling. Samples were drawn with replacements from both the primary and posttraumatic groups, with the sample size set to a smaller group size. Means were calculated for each group, and this process was repeated 1000 times. We then calculated Cohen's d for 1000 pairs of mean values to estimate the effect size using the compute_effsize function with the parameter eftype = 'cohen' from the pingouin library.[28] For all comparisons, we conducted a Mann–Whitney *U* test, with insignificant comparisons labeled with asterisks.

To account for the observed effect of age, we performed the same analysis using age-aligned samples. For each age that appeared in both the primary and posttraumatic groups, one random patient was selected from each group, ensuring that only one patient from each group was chosen for each overlapping age. This process was repeated for all ages common to both groups, resulting in pairs of patients of unique ages. This method ensured that the samples from the two groups shared the same age distribution, allowing for a more accurate comparison by controlling for age as a confounding factor.

2.11. Analysis of single-stranded DNA secondary structure and double-stranded DNA physicochemical properties

We folded DNA to examine how the 189A > G and 408T > A variants impacted mtDNA structure. We utilized unafold[29] with default parameters to predict the secondary structure, and the ionic conditions were set at Na 30 mM and Mg 0.5 mM for normal mitochondria and Na 11.5 mM and Mg 0.5 mM for perforated mitochondria; the minimum and maximum values of ionic conditions for mitochondria were set at Na 5 mM and Mg 0.5 mM and Na 50 mM and Mg 0.5 mM, respectively.[30] To predict the intrabase pair features for double-stranded DNA, we utilized the Deep DNAshape Webserver[31,32] with default settings.

3. Results

3.1. Description of the osteoarthritic cohort

In this study, 106 samples from 105 volunteers (average age 64.25 ± 10.59 years; Supplementary File S1), comprising 75 women and 30 men (for additional information about the patients, see Supplementary Text S1), were analyzed. All participants had been diagnosed with stage 3 gonarthrosis (coxarthrosis) at admission — 13 with posttraumatic osteoarthritis and 92 with primary osteoarthritis (for information about the epidemiology of osteoarthritis, see Supplementary Text S2). Unlike primary osteoarthritis, which results from age-related inflammatory degeneration of cartilage tissue, posttraumatic osteoarthritis develops due to mechanical joint damage within 3–5 years of an injury.[33,34] The subjects reported a disease history of 5–10 years, during which they regularly used various NSAIDs for pain management, as prescribed by their therapists. The most commonly used NSAIDs were indomethacin and ketoprofen (selective inhibitors of cyclooxygenase-1, COX-1), ibuprofen and diclofenac (nonselective inhibitors of both COX-1 and COX-2), and nimesulide (a selective COX-2 inhibitor). Occasionally, patients had exceeded the recommended doses or extended the treatment duration beyond the prescribed limits (based on personal communication with patients).

In the cohort, aside from osteoarthritis, the most common health conditions were circulatory system issues, with 62 patients (56.88 %) reporting conditions such as hypertension, ischemic heart disease, and varicose veins. Digestive system diseases followed, affecting 59 patients (54.13 %), primarily with various forms of gastritis. Endocrine, nutritional, and metabolic disorders were present in 19 patients (17.44 %), including type 2 diabetes in 12 patients (11.01 %) and type 1 diabetes in four patients (3.67 %). Neoplasms, including breast tumors and gastrointestinal polyps, were found in five patients (4.59 %). Diseases of the genitourinary system affected 4.59 % of the volunteers, while musculoskeletal disorders were noted in three patients (2.76 %). Chronic infectious diseases were reported by two patients (1.84 %) — specifically, chronic hepatitis and respiratory conditions in remission. Additionally, there were isolated cases of nervous system, blood, and ophthalmologic disorders. The most common combination of pathologies was stage 2 hypertension with a risk degree of 2–3 and chronic gastritis in remission.

3.2. Identification of muscle-specific m.189A > G and m.408T > A variants in the osteoarthritic cohort

Following NGS analysis of our samples, we identified two somatic variants associated with skeletal muscles: m.189A > G and m.408T > A.[5,10] Using a relaxed SNP calling filter, we found that 72 of the 105 patients had at least one of these variants. Of these patients, 56 had the m.189A > G variant, 43 had the m.408T > A variant, and 27 had both the m.189A > G and m.408T > A variants. When we applied a stricter filter, 61 of 105 patients still had at least one variant. In this case, 41 had m.189A > G, 39 had m.408T > A, and 20 had both m.189A > G and m.408T > A (for a graphical representation, see Supplementary Fig. S1). These variants were present in 83 mtDNA haplotypes of the study cohort (see Fig. 1, Supplementary Fig. S2, and the Haplogroup column in Supplementary File S1), so they were unrelated to the population variants. The diverse haplogroups were attributed to the specifics of the cohort's patients; that is, the population in the region where the study was conducted was composed of immigrants from different geographical areas.

It has been shown that these variants are positively selected in muscle and other postmitotic tissues.[5,16] Our survey of the two biggest datasets of human somatic mutations — TCGA (cancerous)[35] and GTEx (healthy tissues)[36] — revealed a low frequency of the m.189A > G variant. In the TCGA dataset, instances of m.189A > G were found in the prostate (four of 193 samples), pancreas (three of 257), breast (two of 198), esophagus (two of 93), central nervous system (two of 144), kidney (two of 178), liver (two of 294), bone/soft tissue (one of 67), stomach (one of 63), and ovary (one of 103). In the GTEx dataset, m.189A > G was noted in the adrenal gland (one of 83), skeletal muscle (one of 81), and tibial nerve (one of 113). The m.408T > A variant was not detected in either of these datasets. While the GTEx dataset showed a preference for the presence of the m.189A > G variant in postmitotic tissues, this trend was likely absent in TCGA due to its occurrence in several rapidly proliferating tissues (stomach, esophagus, and breast).[37]

Interestingly, by analyzing gnomAD (v3) and HelixMT, we found that both variants could exist in homoplasmic form at low population frequencies, indicating they can be transmitted through the germline (m.189A > G: gnomAD = 0.077, HelixMT = 0.034; m.408T > A: gnomAD = 0.002, HelixMT = 0.003). Given that these variants likely do not have a strongly deleterious effect (although they may be mildly deleterious) when present throughout all tissues, we decided to investigate them further. Our goal was to understand the dynamics and potential associations of these variants with patient phenotypes.[35]

3.3. No significant difference in the variant allele frequency of m.189A > G and m.408T > A between the osteoarthritic and Li et al. (2015) cohorts

Comparing the osteoarthritic cohort with the control cohort from the general population,[5,10] we observed no significant differences in the dynamics of the two variants (Fig. 2), despite the strongly differing nature of the cohorts. The osteoarthritic cohort consisted of patients with stage 3 gonarthrosis or coxarthrosis with various comorbidities, whereas the Li et al. (2015) cohort included postmortem samples from a random population without medically verified gonarthrosis or coxarthrosis. Although the variant dynamics were generally similar across both cohorts (Fig. 2), the osteoarthritic cohort did not exhibit an age-related increase (except for a marginally significant trend; see Fig. 2D) in allele frequencies, as reported in several studies.[5,10,38] This discrepancy may have been due to factors such as a low sample size, narrow age intervals, or the health status of the osteoarthritic cohort, including long-term NSAID usage (see Discussion).

To further demonstrate the equivalence of the observed dynamics of the m.189A > G and m.408T > A variants between the osteoarthritic and the Li et al. (2015) cohorts, we performed a nonparametric four-field matrix analysis (see Methods). This was based on the number of samples with high and low VAF across several age intervals (50–60 years, 60–70 years, and 70–80 years). Consistent with our initial analysis (Fig. 2), no significant differences were observed between the cohorts (Supplementary Fig. S3).

3.4. Phenotypic variations among carriers of different mtDNA variants: clear age differences; other variations are potentially age related

To investigate the potential associations between patient phenotypes and mtDNA heteroplasmy — the two variants of interest and any other variants in CR — we divided the osteoarthritic cohort into five mutually exclusive subsamples of similar size: (1) "189+,408−CR+/−," meaning carrier of 189 ("+" sign) and non-carrier of 408 ("−" sign), irrespective

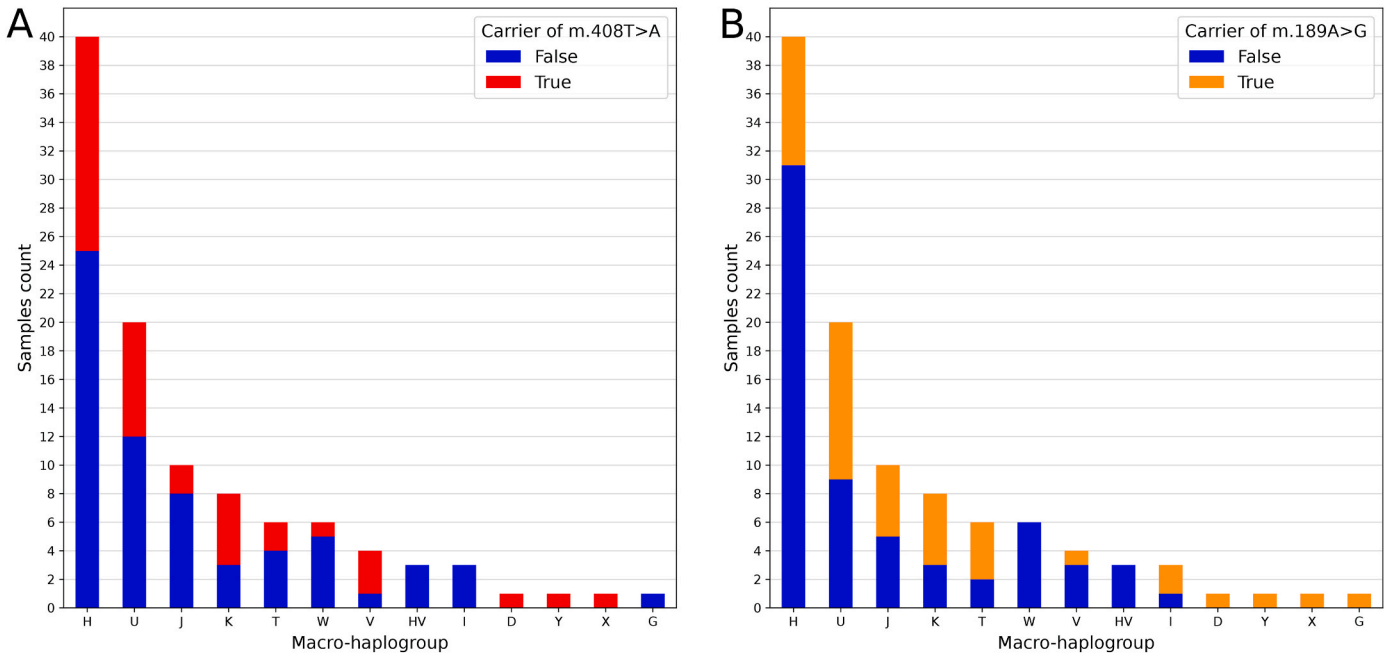

Fig. 1. Distribution of the m.408T > A (A) and m.189A > G (B) variants across macro-haplogroups in the study cohort (sample counts shown after stringent variant filtration). The m.189A > G variant was not observed in haplogroups W and HV (chi-square test: p = 0.02, n = 104; significance remained even after excluding low-abundance haplogroups D, Y, X, G).

of the presence or absence of variants in CR ("+/−" sign); (2) "189−,408+,CR+/−"; (3) "189+,408+,CR+/−"; (4) "189−,408−,CR+"; and (5) "189−,408−,CR−" (see Table 1). Next, we compared the phenotypes of each of these subsamples with the entire cohort. Due to the limited sample size, we employed a nonparametric randomization procedure. We calculated the sum of the trait of interest (e.g., age) for each subsample and compared it to the distribution of sums generated through 10,000 random samplings with the replacement of patients from the entire cohort. Table 1 shows the fraction of comparisons when the expected value was lower than the observed value (hereafter, the percentile of the observed values among the distribution of expected values). For example, in 97.52 % of the random samplings, the observed age in Subsample 3 was higher than the expected age, indicating that patients in this subsample were significantly older than those in the overall cohort.

Considering a 5 % threshold, where observed values fall below the 5th percentile or above the 95th percentile of expected values, we highlighted several trends, marked in bold in Table 1 and Supplementary Table S1. Age differences were notable, with Subsample 1 being younger and Subsamples 2 and 3 being older than the overall dataset. In addition to age, we observed the following trends: Sample 1 showed high leukocyte, ALT, and AST levels; Subsample 2 exhibited relatively low ALT, creatinine, and blood pressure levels; Subsample 3 displayed lower AST values but higher ESR levels; Subsample 4 had high AST values; and Subsample 5 showed high creatinine levels. It is important to emphasize that, despite these variations, all physiological parameters remained within normal reference ranges and that age may have had a significant impact on these measures. Altogether, there were no strong differences between the subsamples that could not be explained by age variation.

3.5. Phenotypic variations among the primary osteoarthritic and posttraumatic (n = 13) subcohorts: clear age differences; other variations are potentially age related

Next, we analyzed the phenotypic differences between the primary osteoarthritic (n = 92) and posttraumatic (n = 13) subcohorts of patients from our osteoarthritic cohort. We compared these groups using Cohen's d statistic, which is an effect size indicating the standardized difference between two means (Table 2 and Supplementary Table S2). A high Cohen's d value reflects an increased mean in the group of interest (the primary osteoarthritic subcohort in our case), while a low value reflects a decreased mean. Among all the phenotypes we examined, we also evaluated the variant allele frequencies of both variants, considering them molecular phenotypes of mtDNA. Notably, these variants showed the most pronounced differences: the patients with primary osteoarthritis exhibited significantly higher levels of heteroplasmy for the m.189A > G and m.408T > A variants than those with posttraumatic osteoarthritis (see Table 2). Expectedly, the primary osteoarthritis patients were significantly older (by more than 9 years, on average) than the posttraumatic patients, and this difference may explain other observations, including the increased VAFs of both mtDNA variants. The younger age of the posttraumatic osteoarthritis patients can be explained by their increased physical activity (e.g., participation in sports) and involvement in car accidents, both of which often lead to knee or hip injuries. The older age of patients with primary osteoarthritis, along with their potentially increased inflammatory status and higher usage of NSAIDs (see Discussion), may have contributed to their trend of having elevated levels of bilirubin, cholesterol, ALT, blood pressure, and body mass index (BMI) (Table 2).

Taken together, the osteoarthritic subcohorts under analysis showed a significant relative difference in BMI and liver function (total bilirubin and ALT) parameters. These differences may have been associated with the long-term use of hepatotoxic NSAIDs. The dystrophic phenomenon in muscle tissue could be attributed to the relative decrease in creatinine levels observed in many patients.[39,40] Taking all this into account, it can be concluded that the patients in the studied cohort experienced prolonged physiological stress (pain syndrome).

3.6. Phenotypes associated with mtDNA variants within a subcohort of primary osteoarthritic patients: slight age differences

To determine whether the presence of mtDNA variants (m.189A > G and m.408T > A) was associated with phenotypic changes, we divided

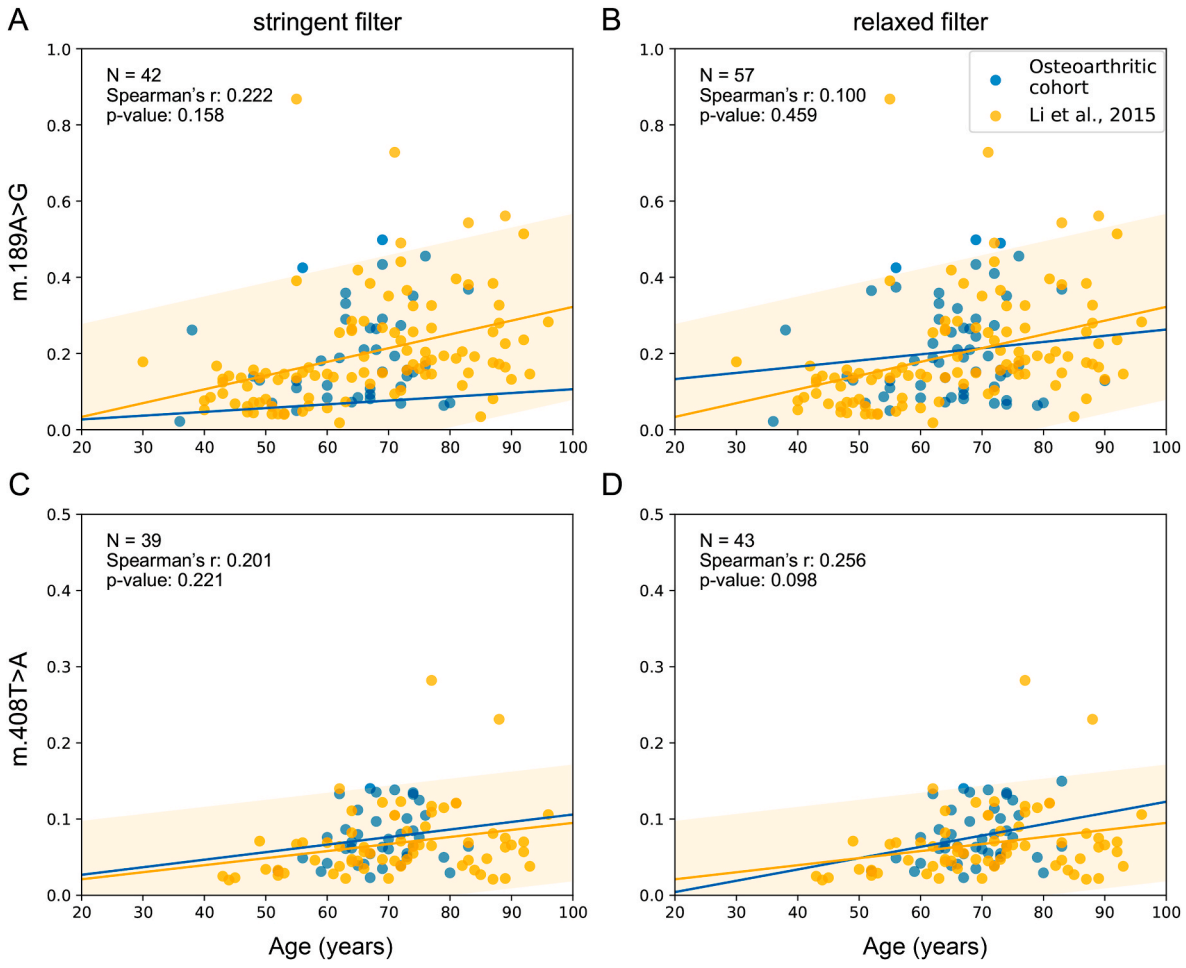

Fig. 2. Scatter plots showing the variant allele frequencies as a function of age. Variation types (m.189A > G and m.408T > A) are presented in rows, while data filtration types (stringent or relaxed) are shown in columns. Orange dots and linear regression lines represent data from Li et al. (2015), with orange shading indicating a 90 % confidence interval. Blue dots and regression lines represent data from the osteoarthritic cohort.

Table 1
Phenotypic variations among five subsamples carrying different mtDNA variants. Each cell shows the percentile and average values (the full table is available in Supplementary Table S1).

Percentiles and average phenotypic values for five subsamples (see Supplementary Table S9 for the units of measurement)	(1) 189+,408−, CR+/− (carriers of m.189A > G; n = 22)	(2) 189−,408+, CR+/− (carriers of m.408T > A; n = 19)	(3) 189+,408+,CR+/− (carriers of m.189A > G and m.408T > A; n = 20)	(4) 189−,408−,CR+ (noncarriers of m.189A > G or m.408T > A but carriers of variants in the control region; n = 19)	(5) 189−,408−,CR− (noncarriers of any variants in the control region; n = 22)
Age	**0.0328** **61.0**	**0.9359** **68.21**	**0.9752** **69.05**	0.1445 62.58	0.1212 62.45
Diastolic blood pressure	0.9276 83.55	**0.0274** **75.26**	0.4608 80.65	0.6246 81.58	0.3053 79.55
Leukocytes	**0.976** **7.39**	0.7913 6.97	0.0439 5.91	0.347 6.45	0.4688 6.58
ESR	0.4061 11.23	0.0944 8.95	**0.9796** **16.35**	0.8242 13.84	0.1891 9.95
ALT	**0.9951** **29.69**	**0.0096** **15.88**	0.3795 20.69	0.4015 20.9	0.4408 21.26
AST	**0.9882** **25.63**	0.1202 18.69	**0.0436** **17.79**	0.617 21.77	0.8067 22.82
Creatinine	0.8979 79.95	**0.0313** **61.13**	0.2234 68.23	0.5869 74.26	**0.9688** **83.2**

Table 2
Comparing patients with primary arthritis with those with posttraumatic arthritis (the full table is available in Supplementary Table S2).

Primary arthritis (n = 92); posttraumatic arthritis (n = 13); both sexes	Primary arthritis (mean)	Primary arthritis (SD)	Posttraumatic arthritis (mean)	Posttraumatic arthritis (SD)	Cohen's d
Molecular phenotype, m.189A > G allele frequency (stringent filter, nonzero values only)	0.217682 (n = 34)	0.124739	0.102878 (n = 8)	0.073663	0.977757
Molecular phenotype, m.408T > A allele frequency (stringent filter, nonzero values only)	0.081908 (n = 31)	0.035618	0.04818 (n = 8)	0.01618	1.027222
Age	65.76904	2.811336	56.61306	3.288817	2.99273
Bilirubin	13.85834	1.838364	11.29793	0.850204	1.787737
Monocytes	6.9489	0.697497	5.839103	0.548557	1.768708
BMI	32.85808	1.832978	30.10093	1.711895	1.554661
Cholesterol	5.739273	0.511316	5.176326	0.450643	1.168096
Systolic blood pressure	131.2111	4.085784	126.9475	3.967846	1.05869
ALT	22.4013	4.067884	27.10687	5.213565	−1.00634
SII	465.2145	84.05479	589.1788	139.3461	−1.07729
NLR	1.73154	0.220756	2.074988	0.30488	−1.29037
Neutrophils	55.952130	2.335502	58.941323	2.280756	−1.294981
sLII	1.277904	0.16548	1.617054	0.217138	−1.75684

Note: All Cohen's d values were significant. The significance of Cohen's d for allele frequency values was calculated using Welch's *t*-test.

Table 3
Comparison of primary arthritis patients with m.189A > G and/or m.408T > A variants (carriers) and those without such variants (noncarriers). Both sexes were used for the comparison (the full table is available in Supplementary Table S3).

Carriers, m.189A > G and/or m.408T > A (n = 50); noncarriers (n = 38)	Carriers (mean)	Carriers (SD)	Noncarriers (mean)	Noncarriers (SD)	Cohen's d
Age	67.20121	1.267242	63.8906	1.66163	2.240456
Bilirubin	14.58374	1.117266	13.08435	0.732644	1.587105
Height	163.474	1.618706	165.0904	1.477212	−1.04309
Creatinine	77.76219	2.458339	83.10044	4.410814	−1.49505
sLII	1.203512	0.071615	1.376544	0.097944	−2.0168

Note: All Cohen's d values were significant.

the cohort of primary osteoarthritic patients into two groups: carriers (patients with at least one of the two mtDNA variants of interest; n = 50) and noncarriers (n = 38) (Table 3 and Supplementary S4). In this analysis, four patients were excluded due to low-quality sequencing data. For comparison, we again used Cohen's d statistic, with carriers being the group of interest. Consistent with previous findings, we observed that age was the primary factor explaining the differences between the compared groups: carriers were only slightly older (by 3.3 years, on average), and thus, additional differences may have been influenced by age, but we could not also exclude clinical differences. The bilirubin level in the carrier group was elevated relative to the noncarrier group. This may suggest reduced liver function and signs of an inflammatory reaction compared to volunteers who did not have mutational changes. Both groups had creatinine levels within the reference range. However, the carriers had lower levels, which is an indirect indicator of the development of muscular dystrophies. Both groups had normative values for the leukocyte indices of intoxication (sLII), but the sLII in the noncarrier group was slightly higher, which could have been caused by different doses of NSAIDs. Both groups had elevated levels of leukocyte indices (SII, SIRI, and AISI) compared to

Table 4
Comparison of all primary arthritis patients with the m.189A > G variant and those without this variant (nonmutated) (the full table is available in Supplementary Table S4).

Carriers, m.189A > G (n = 26); noncarriers (n = 34); both sexes	Carriers (mean)	Carriers (SD)	Noncarriers (mean)	Noncarriers (SD)	Cohen's d
BMI	34.30407	0.490609	31.12506	0.585834	5.883528
Weight	92.57961	1.497264	83.18856	1.95313	5.396571
Bilirubin	15.00512	0.330568	13.24791	0.444005	4.489333
Dynamometry, left hand	38.89914	1.363288	26.73875	4.289819	3.820596
Systolic blood pressure	132.6069	1.589936	126.3806	2.013988	3.431665
Dynamometry, average	38.81582	0.778195	28.87144	4.359087	3.17603
Dynamometry to BMI	1.173523	0.057595	0.940849	0.097973	2.895363
Dynamometry, right hand	38.7325	0.26345	31.00413	4.432342	2.461522
ALT	24.62515	2.604628	19.66809	1.273603	2.417911
Creatinine	80.67515	1.55762	74.95723	3.454591	2.133882
Eosinophils	2.437226	0.09561	2.108425	0.230923	1.860474
ESR	17.06637	1.253773	15.00795	1.199691	1.677558
AST	22.50132	1.254299	20.65967	1.131763	1.541643
Neutrophils	56.12322	0.981612	54.97877	1.089543	1.103637
Heart rate	79.57228	1.1997	77.93061	1.816968	1.066304
Age	66.66667	1.42E-14	66.66667	1.42E-14	0*
Monocytes	6.339367	0.192494	6.608555	0.305014	−1.05549
Cholesterol	5.496703	0.144791	5.81613	0.272588	−1.46356
LMR	6.881622	0.192991	7.266699	0.298907	−1.5306
IIR	6.833541	0.227306	7.729603	0.300825	−3.36093
Glucose	5.710693	0.102364	6.19526	0.114116	−4.47018

Note: *Insignificant value.

healthy individuals, suggesting a systemic inflammatory process.

3.7. Phenotypes associated with mtDNA variants within age-matched samples with primary osteoarthritis: BMI, body weight, and muscle strength

Given the age differences observed in all the previous comparisons, which may have obscured potential independent associations between mtDNA variants and phenotypes, we implemented an age-matching procedure (see Methods). This allowed us to control for this crucial factor in the downstream analyses. We repeated the analysis from Table 3 specifically for the m.189A > G variant, comparing carriers (those with the variant) to noncarriers (those without the variant), matched by age (see Table 4 and Supplementary Table S4). Notably, after age matching, several interesting and significant findings emerged (following an arbitrary threshold in absolute values of Cohen's d greater than 2[41]): carriers, compared to noncarriers, exhibited higher BMI and body weight and several indicators of muscle strength (dynamometry tests), bilirubin levels, blood pressure, ALT, and creatinine (see Table 4). Conversely, carriers had decreased IIR and glucose levels (Table 4). It is possible that the increased IIR in both groups was due to the regular use of NSAIDs, which suppress inflammatory reactivity.

The increased BMI, body weight, and muscle strength in carriers, no longer confounded by age, may still have been influenced by sex differences between the compared groups. Since women constituted the majority of our volunteers, we reran the previous analysis (Table 4) to focus solely on women and obtained very similar results (Supplementary Table S5). This confirms that carriers of the m.189A > G variant were indeed associated with higher BMI and muscle strength, independent of age and gender. Additionally, women with the m.189A > G SNP had elevated values of ESR and eosinophils and decreased numbers of leukocytes and IIR. It is possible that these additional differences were not specific. This problem will be resolved as the study group grows over time.

Next, we conducted an age-matched analysis of primary osteoarthritis patients with the m.408T > A variant and observed results highly similar to those with the m.189A > G variant; that is, compared to the noncarriers of m.408T > A, the carriers of m.408T > A exhibited higher BMI; greater muscle strength, as measured by dynamometry proxies; and several other parameters (see Table 5 and Supplementary Table S6). It is of interest that in the noncarrier group, the ESR level was near the upper limit of the norm and the values of a number of leukocyte indices (sLII, PLR, SIRI, NLR, and SII) were higher. This could indicate a higher level of inflammation in nonmutated volunteers.

The same analysis — age-matched comparisons of carriers versus noncarriers of the m.408T > A variant primary among osteoarthritis patients — although focusing solely on women (see Supplementary Table S7), confirmed the key trends obtained for both sexes (Table 5): increased weight, BMI, and muscle strength. Additionally, the levels of monocytes, basophils, and lymphocytes were somewhat higher in carrier women, which was reflected in the lower values of "inflammatory" leukocyte indices, confirmed by the low ESR level values. It is possible that the identified patterns reflected the lower intensity of inflammatory processes in female volunteers with m.408T > A. Thus, it can be presumed that women with a variant at position 408 additionally have a higher degree of preservation of inflammatory processes than women without a variant.

Overall, age-matched analyses revealed a robust and significant increase in BMI, body weight, and muscle strength in carriers of the mtDNA variants. These findings were consistently confirmed in analyses focusing solely on women.

Taken together, patients with the m.189A > G and m.408T > A SNPs may have a physiologic compensatory effect, primarily at the muscle level, due to the presence of heteroplasmy of these SNPs, as indicated by the relatively high dynamometry parameters. This may be a link to a higher rate of muscle recovery with the studied heteroplasmy during hypoxia (similar to the hypercompensatory effects experienced by climbers after high-altitude acclimatization).

Table 5
Comparison of all primary arthritis patients with the m.408T > A variant and those without the variant (nonmutated) (the full table is available in Supplementary Table S6).

Carriers, m.408T > A (n = 28); noncarriers (n = 37); both sexes	Carriers (mean)	Carriers (SD)	Noncarriers (mean)	Noncarriers (SD)	Cohen's d
Bilirubin	15.74177	0.457036	12.5129	0.589117	6.124237
Dynamometry, average	35.61161	1.641779	24.61937	3.250946	4.268374
Dynamometry, left hand	33.62494	1.995326	23.18293	3.015596	4.083904
Dynamometry, right hand	37.59829	1.738625	26.05582	3.795583	3.909978
Lymphocytes	35.99623	0.551478	32.7182	1.105824	3.751563
Red blood cells	4.68718	0.014939	4.541445	0.060905	3.286559
Weight	91.30405	2.265588	85.38197	2.090568	2.716756
Dynamometry to BMI	1.071564	0.090235	0.796791	0.118825	2.604404
Height	164.447	0.576083	162.2991	1.360564	2.055944
Basophils	0.696295	0.069905	0.564662	0.065507	1.943168
Hemoglobin	135.1293	0.993532	132.1956	2.235676	1.69586
Monocytes	7.271603	0.242877	6.812836	0.319775	1.615713
BMI	33.4984	0.875973	32.33464	0.5666	1.577575
LMR	6.042003	0.170225	5.737489	0.361332	1.078183
Age	69.84211	1.42E-14	69.84211	1.42E-14	0*
IIR	5.625253	0.215946	6.077755	0.428729	−1.33308
AST	20.815	0.397404	22.77225	1.325764	−1.99991
PLR	112.1177	4.067615	127.6324	10.08466	−2.01774
Leukocytes	6.594294	0.103882	7.129192	0.351253	−2.06518
SIRI	0.765408	0.041643	0.968378	0.1255	−2.17082
Creatinine	77.49483	1.666217	83.58454	3.533922	−2.20427
ALT	19.20105	0.617316	22.96573	2.185284	−2.34458
Thrombocytes	245.6344	6.769874	271.0642	13.29602	−2.41035
AISI	200.8654	12.77835	303.6904	52.81722	−2.676
Eosinophils	2.124234	0.145479	2.636728	0.227242	−2.68614
Neutrophils	54.48756	0.876089	57.36109	1.116393	−2.86362
ESR	13.99036	1.414914	18.03254	1.406021	−2.86583
NLR	1.547519	0.071228	1.835783	0.120406	−2.91405
SII	397.8387	20.94057	529.6712	58.00089	−3.02341
sLII	1.084879	0.060297	1.385064	0.065725	−4.75958

Note: *Insignificant value.

3.8. Potential effects of the m.189A > G and m.408T > A variants on mtDNA dynamics

The dynamics of the m.189A > G and m.408T > A SNPs may be governed by a balance of intra- and intercellular selection processes. Specifically, in postmitotic tissues in which cellular turnover is minimal, the primary selection pressure is intracellular and can be closely related to changes in the structure of the L-strand promoter (LSP) of mtDNA (m.408T > A) (Fig. 3A and E) or the OH1 origin of replication of the H-strand of mtDNA (Fig. 3A and D).[16,42] To mechanistically understand why these variants might lead to increased mtDNA replication or decreased mtDNA degradation, we delved into their potential effects on mitochondrial DNA structure and functionality, with and without taking into consideration the effect of NSAIDs (mitochondrial membrane perforation) on DNA structure. This investigation involved the computational modeling of single-stranded DNA structures using Unafold, whereby we adjusted the ionic conditions to simulate different mitochondrial environments, and the computational prediction of double-stranded DNA (dsDNA) properties using the Deep DNAshape webserver (Supplementary Table S8).[31,32] By exploring the m.189A > G variant effect on polymerase gamma (POLG) and/or mtSSB affinity to the OH1 region of mtDNA, and by studying the potential affinity of POLRMT and/or TFAM and TFB2M (two essential transcription cofactors[42]; Fig. 3C) in the context of the m.408T > A variant at the LSP region of mtDNA, we aimed to uncover the underlying mechanisms allowing these variants to persist and expand in postmitotic tissue types, potentially influencing health status and cellular aging.

- m.189A > G

There were no distinctions between the normal and mutated structures within the 110–212 bp region of the H-strand in the membrane environment perforated by NSAIDs (Supplementary Fig. S4); however, we found huge differences between them in the L-strand (Fig. 3B and C and Supplementary Fig. S5), especially in terms of critical ionic conditions (Supplementary Fig. S6). As shown in Fig. 3B and C, in the single-strand state, the 189A > G variant leads to a reduction in hairpin length, which in turn decreases hairpin stability, thereby facilitating an easier passage for enzymes. We found significant modifications in the dsDNA properties of the mutated OH1 region, especially the propeller twist (Fig. 3F; additional information in Supplementary Figs. S10, S11, and S14 and Table S9). This information is intriguing, as changes in flexibility in this region can result in changes in POLG and/or mtSSB affinity to the origin of H-strand replication.[43]

- m.408T > A

Although there were no distinctions between the normal and mutated structures within the 364–441 bp region of the L-strand in the membrane environment perforated by NSAIDs (Supplementary Fig. S7), we found significant differences between them in the H-strand (Supplementary Fig. S8). However, the differences between normal and mutated structures within the L-strand began to occur in critical ionic conditions (Supplementary Fig. S9). Furthermore, we discovered a widening of minor groove width in the mutated LSP region (Fig. 3G) as well as changes in the shear distance and nucleotide opening angle in dsDNA (additional information in Supplementary Figs. S12, S13, and S14 and Table S9), which is intriguing, considering that minor groove width values in protein-bound DNA are significantly wider than in free DNA.[44] The 408 position was located near the transcription start site of the LSP and at the core of the transcription initiation complex (Fig. 3A and E[45]). Thus, the change in the 408 position is likely to have affected the overall transcriptional function of mitochondria.

Overall, the connection between the molecular properties of the m.189A > G and m.408T > A SNPs and their expression should be rooted in their effect on the replication of the mtDNA H-strand and the effectivity of transcription from the L-strand promoter, respectively.

3.9. Assessing the relationship between the mtDNA copy number and the presence of the m.189A > G and m.408T > A variants

To test the direct effect of the m.189A > G and m.408T > A variants on the mtDNA copy numbers of the osteoarthritic cohort (Table 6), which can be interpreted as an expression of these variants, we compared the controls (posttraumatic arthritis patients) and cases (primary arthritis patients) in all possible pairwise combinations (Table 6). We restricted our analysis to a subset of our osteoarthritic cohort comprising seven posttraumatic arthritis patients and 34 primary arthritis patients. We also considered differences in the mean ages of the compared subgroups. Table 6 demonstrates at least two clear trends in pairs of patient groups of comparable ages (shown in bold type in Table 6): (1) the number of mtDNA copies was significantly higher in the primary arthritis patients who had only the m.189A > G variant than in those with both the m.189A > G and m.408T > A variants (comparison #8); (2) the number of mtDNA copies in the posttraumatic arthritis patients with both m.189A > G and m.408T > A variants was significantly lower than in the primary arthritis patients with both m.189A > G and m.408T > A variants (comparison #12). The primary cause of the first trend can be traced back to the fact that position 189 is situated in the OH1 region, which is the starting point for H-strand replication, while position 408 is situated in LSP, which is the promoter for L-strand transcription; therefore, the variant in this position can compensate for the effect of the variant in position 189 (comparison #8). However, considering the second trend, we cannot exclude the possibility that the mtDNA copy number additionally rises during primary arthritis in patients with these variants (comparison #12).

4. Discussion

We proposed a population genetic hypothesis that provides a parsimonious explanation for all observed data from both our research and other studies. The two variants in question are rarely observed in proliferative tissues but are more common in postmitotic tissues. This suggests two potential scenarios: (1) a slightly deleterious scenario in all tissues, where the variants are selfish and consistently associated with a decrease in cellular fitness but can still reach high frequencies in postmitotic tissues due to weak intercellular selection, and (ii) a beneficial scenario in skeletal muscles only, where the variants enhance the fitness of muscle cells (possibly by boosting mtDNA replication) and remain effectively neutral or even deleterious in other tissues. Below, we focus primarily on the first scenario, as the literature provides close and analogous examples. The second scenario remains open to future investigation.

According to the first, slightly deleterious scenario in all tissues, within a host cell, these variants may be selfish; that is, they may confer an intracellular advantage to mtDNA due, for example, to a faster replication rate, whereas at the intercellular level, they may reduce the overall functionality of the cell. In highly proliferative tissues, where intercellular selection is strong, cells carrying such mtDNA variants are selected against due to their lower fitness. In contrast, in postmitotic tissues, where intercellular selection is weak or absent, these selfish variants can multiply, reaching high allele frequencies within individual host cells. This interplay between intra- and intercellular selection reflects the dynamics of somatic mtDNA deletions, a well-known hallmark of aging in neurons and skeletal muscles.[47] Although these deletions are common in postmitotic tissues, they are rarely detected or able to reach high allele frequencies in proliferative tissues. Following the logic behind the selfish nature of the two SNPs, it is reasonable to assume that host cells (cells of skeletal muscles) carrying these variants should experience a fitness decline compared to cells without these variants. Investigating this potential decline in fitness presents an exciting prospect for future research in single-cell biology. This approach resembles

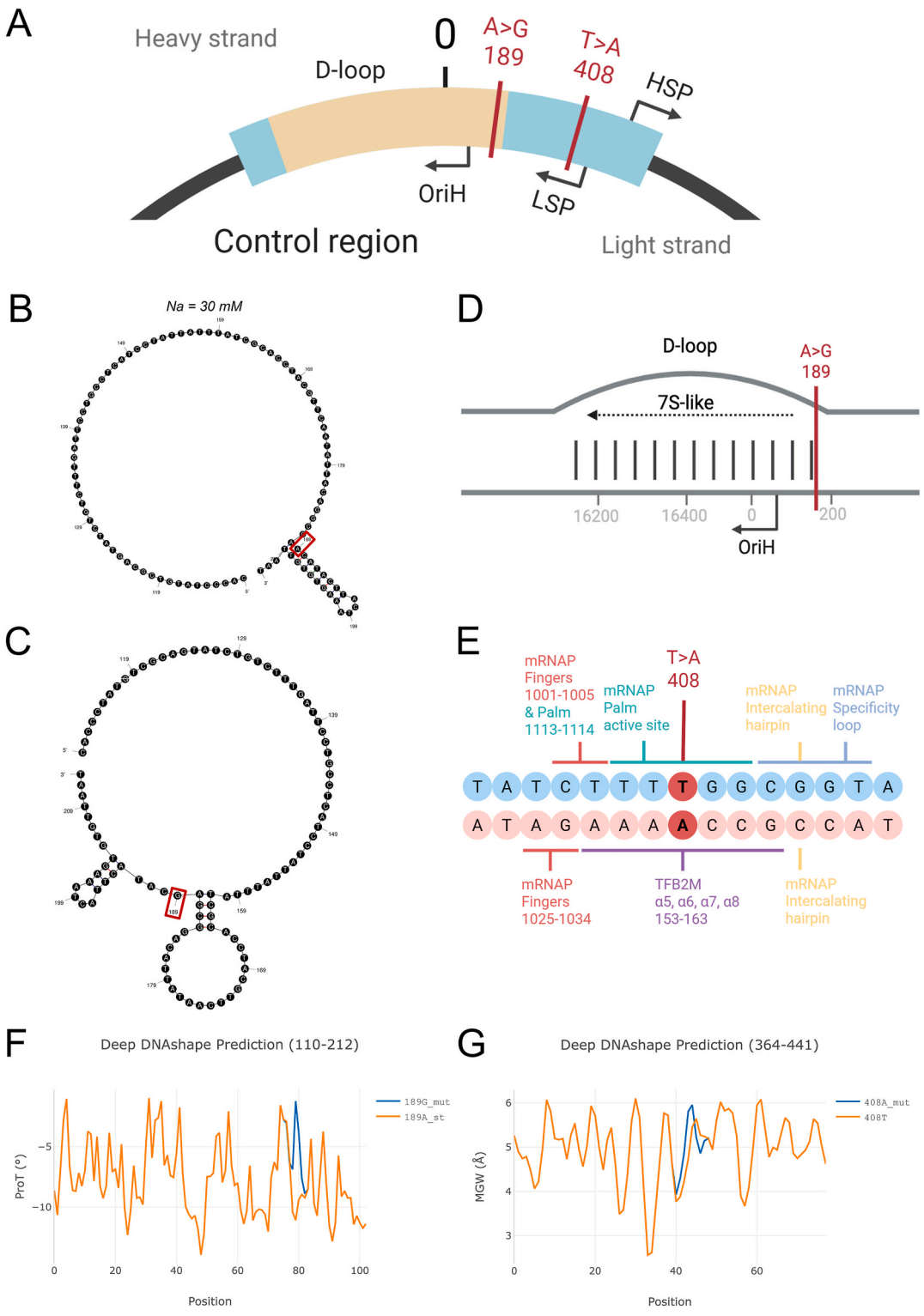

Fig. 3. Possible effects of m.189A > G and m.408T > A on mtDNA replication and transcription. (A) The positions of the m.189A > G and m.408T > A variants relating to H-strand (HSP) and L-strand promoters (LSP), H-strand origin of replication (OriH), and D-loop. (B) Predicted secondary structure for the 110–212 bp region (L-chain) in normal mitochondria (ionic condition: Na = 30 mM) without substitutions (dG = −1.36 kcal/mol) and (C) with m.189A > G substitution (dG = −0.55 kcal/mol). (D) The m.189A > G variant located at the beginning of the D-loop in a single-stranded state may affect the formation of a 7S DNA third-stranded structure.[46] (E) The m.408T > A variant is located in region where TFB2M and mRNAP Palm proteins bind with DNA.[45] (F) Predicted propeller twist (ProT) parameter double-stranded DNA 110–212 region, intra-base pair features. Mean ProT angle with substitution: −5.4545°, without substitution: −7.7021°. (G) Predicted minor groove width parameter double-stranded DNA 364–441 region, intra-base pair features. Mean MGW with substitution (blue line): 5.0279 Å, without substitution (orange line): 4.8226 Å.

Table 6
Comparison of mtDNA copy numbers between various patient subgroups.

	(1) Mean	(1) StDev	(2) Mean	(2) StDev	Cohen's d
#1: All controls (1, n = 7) vs. all cases (2, n = 34) Age: (1) 56.3 ± 14.3 vs. (2) 68.3 ± 7.5	1030.358	1058.386	1657.824	1337.559	−3.01768
#2: All controls (1, n = 7) vs. cases_189 (2, n = 25) Age: (1) 56.3 ± 14.3 vs. (2) 67.1 ± 8.3	1030.358	1058.386	1633.973	1126.403	−2.97012
#3: All controls (1, n = 7) vs. cases_408 (2, n = 23) Age: (1) 56.3 ± 14.3 vs. (2) 69.8 ± 7.0	1030.358	1058.386	1529.218	1371.296	−2.01421
#4: All controls (1, n = 7) vs. cases_189&408 (2, n = 14) Age: (1) 56.3 ± 14.3 vs. (2) 68.7 ± 8.5	1030.358	1058.386	1403.949	971.6731	−1.62866
#5: All cases (1, n = 34) vs. cases_189&408 (2, n = 14) Age: (1) 68.3 ± 7.5 vs. (2) 68.7 ± 8.5	1657.824	1337.559	1403.949	971.6731	1.382908
#6: All cases (1, n = 34) vs. cases_189 (2, n = 25) Age: (1) 68.3 ± 7.5 vs. (2) 67.1 ± 8.3	1657.824	1337.559	1633.973	1126.403	0.143718*
#7: All cases (1, n = 34) vs. cases_408 (2, n = 23) Age: (1) 68.3 ± 7.5 vs. (2) 69.8 ± 7.0	1657.824	1337.559	1529.218	1371.296	0.705894*
#8: All cases_189 (1_excluding_2, n = 11) vs. cases_189&408 (2, n = 14) Age: (1) 64 ± 6.6 vs. (2) 68.7 ± 8.5	2555.729	1632.878	1403.949	971.6731	**4.245384**
#9: All cases_408 (1_excluding_2, n = 9) vs. cases_189&408 (2, n = 14) Age: (1) 71.8 ± 3.0 vs. (2) 68.7 ± 8.5	1121.992	1110.213	1403.949	971.6731	−1.25854
#10: Controls_189 (1, n = 6) vs. all cases_189 (2, n = 25) Age: (1) 54.8 ± 15.1 vs. (2) 67.1 ± 8.3	688.3901	601.5831	1633.973	1126.403	−4.82795
#11: Controls_408 (1, n = 4) vs. all cases_408 (2, n = 23) Age: (1) 66.3 ± 5.4 vs. (2) 69.8 ± 7.0	1200.222	1267.513	1529.218	1371.296	−1.2102
#12: Controls_189&408 (1, n = 3) vs. cases_189&408 (2, n = 14) Age: (1) 66.7 ± 6.5 vs. (2) 68.7 ± 8.5	572.9068	220.7655	1403.949	971.6731	**−3.54409**

Note: *Insignificant value.

studies on human substantia nigra neurons in which respiratory chain deficiencies in individual neurons have been linked to the high burden of somatic mtDNA deletions.[48]

What is the potential mechanism behind the selfish clonal expansion of mtDNA with the two SNPs within muscle cells? A useful analogy can be drawn from the well-known dynamics of a rheostat switch from transcription to replication — the m.302A > AC variant, which is the most common heteroplasmy in human blood.[49] The m.302AC allele strengthens the formation of a G-quadruplex structure on the heavy strand, acting as a more effective barrier to RNA polymerase and thereby disrupting transcription in favor of replication.[50,51] This can promote the clonal expansion of the m.302AC variant in somatic tissues. Although evidence is limited, we propose that the m.T408A variant reduces transcriptional efficiency while the m.A189G variant enhances replication. Assuming that replication and transcription are mutually exclusive in mtDNA,[51] these variants might act as switches between these processes, either together or independently.

Interestingly, despite the potential deleterious effects proposed in the framework of the first scenario, both variants can be transmitted through the germline and exist in a homoplasmic state. The m.A189G variant is present in 3–8 % of humans. MitoMap reports 3–5 %[52] and serves as a marker variant for many haplogroups,[53] with frequencies of 0.077 in gnomAD and 0.034 in HelixMT. This suggests that any negative effects are likely only mildly deleterious, highlighting the need for a detailed investigation of carriers with these homoplasmic variants.

Additionally, compensatory variants and/or physiological responses to permanent stress could mitigate these effects. The studied cohort had preoperative use of NSAIDs among their characteristics. The majority of patients experienced severe pain and had probably taken NSAIDs for a long period of time (longer than the course prescribed by the doctor), even exceeding the recommended doses. NSAIDs have previously been shown to affect the functioning of mitochondria and the mutational processes of mtDNA. The functioning of the electron transport chain can be disrupted by NSAIDs, leading to depolarization through electron or proton leakage, resulting in lower efficiency of oxidative phosphorylation processes.[54–56] They can cause Ca2+ efflux, thereby changing the permeability of the mitochondrial membrane.[57,58] At the same time, the functioning of mitochondria can be affected more or less by different substances in the NSAID group. In one study, indomethacin had a direct effect on SIRT3, the main mitochondrial deacetylase for structural and functional proteins, such as SOD2 and OGG1.[59,60] Eventually, mitochondrial oxidative stress causes an increase in reactive oxygen species, which leads to the oxidation of mtDNA and the subsequent production of 8-oxo-guanine.[61] Indomentacin can also speed up mitochondrial fission, resulting in the accumulation of damaged mitochondria with excessive hyperactivation of the PKCζ-p38 MAPK-DRP1 pathway, which is further mediated by a positive feedback loop and results in mitochondrial hyperfission.[62] In vivo, NSAIDs have been shown to inhibit skeletal muscle protein synthesis and decrease the rate of mitochondrial protein synthesis after exercise.[63] Impaired mitophagy and apoptosis, or induction of mtDAMP, are some of the structurally higher levels whereby these processes, either individually or collectively, can manifest at a structurally higher level as inflammation.[61] Taken together, detailed phenotypic analyses of carriers from large biobanks, such as the UK Biobank,[49] may offer future insights into the potential effects of these variants in the homoplasmic state and in cases of various clinical characteristics. Alternatively, further analysis of the effect of mitochondrial compensatory/covariation mutation in evolution could provide valuable insights.

The most intriguing finding of this study is the potential association between these variants and increased BMI, body weight, and muscle strength (evaluated by dynamometry), which can be explained by both proposed scenarios. Increased BMI is known to be associated with hypertrophy of skeletal muscles, especially type II fibers (fast-twitch fibers used for strength and power, which rely on glycolysis instead of oxidative phosphorylation).[64] According to the first scenario, selfish mtDNA variants might clonally expand more effectively under these conditions, possibly due to the increased volume of hypertrophic skeletal muscles or their glycolytic activity. The second scenario suggests that these variants could be beneficial, aiding individuals with a high BMI in managing extra weight and enhancing muscle strength. Future studies investigating which specific muscle fibers (type I, responsible for endurance and based on oxidative phosphorylation, or type II, responsible for rapid responses and based on glycolysis) are prone to accumulate these variants could provide insights into their dynamics.

5. Conclusions

We confirmed the accumulation of the m.189A > G and m.408T > A variants in human skeletal muscle within our osteoarthritic cohort. The variation dynamics did not differ significantly from those observed in a control population,[5] with both variant dynamics and the majority of patient phenotypes largely explained by age. However, controlling for age and gender (in a women-only cohort), we found that carriers of the m.189A > G or m.408T > A variants consistently exhibited higher BMI, body weight, and muscle strength than noncarriers. Additionally, we revealed that the molecular effects of the m.189A > G and m.408T > A SNPs are connected to mtDNA replication and transcription, which are involved in shaping the mtDNA copy number. This intriguing observation suggests two possible explanations: either these variants are a consequence of clonal expansion (expanding more rapidly in the hypertrophic muscle fibers of patients with higher body weight) or they may play a causative role, influencing these traits through unknown mechanisms. Further detailed research is needed to better understand the dynamics and potential impacts of these variants.

CRediT authorship contribution statement

Valeria Lobanova: Writing – review & editing, Writing – original draft, Project administration, Investigation, Formal analysis, Data

curation. **Ivan Kozenkov:** Validation, Project administration, Methodology, Investigation, Data curation. **Eldar Khaibulin:** Writing – original draft, Visualization, Software, Formal analysis, Data curation. **Maria Tatarkina:** Investigation, Data curation. **Bogdan Efimenko:** Formal analysis. **Viktoria Skripskaya:** Writing – original draft, Visualization, Formal analysis. **Akhsarbek H. Dzhigkaev:** Resources, Methodology, Investigation. **Anastasia S. Krylova:** Resources. **Anastasia V. Prokopenko:** Resources. **Stepan V. Toshchakov:** Resources. **Andrey Goncharov:** Writing – original draft, Validation, Project administration, Methodology, Data curation. **Konstantin Popadin:** Writing – review & editing, Writing – original draft, Supervision, Resources, Project administration, Funding acquisition, Conceptualization. **Konstantin V. Gunbin:** Writing – review & editing, Writing – original draft, Visualization, Validation, Supervision, Software, Project administration, Methodology, Funding acquisition, Formal analysis, Conceptualization.

Consent to participate

All authors have read and agreed to the published version of the manuscript.

Informed consent statement

Informed consent was obtained from all subjects involved in the study. Written informed consent has been obtained from the patients to publish this paper.

Ethical approval

The study was conducted in accordance with the Declaration of Helsinki by the World Medical Association and the Guideline for Good Clinical Practice by the International Council for Harmonisation, and it was approved by the Independent Ethics Committee of the Clinical Research Center of Immanuel Kant Baltic Federal University (protocol code 25 from June 30, 2021).

Institutional review board statement

The study was conducted in accordance with the Declaration of Helsinki by the World Medical Association (WMA) and the Guideline for Good Clinical Practice by International Council for Harmonisation (ICH GCP), and approved by the Independent Ethics Committee of Clinical Research Center of the Immanuel Kant Baltic Federal University (protocol code 25 from June 30, 2021).

Funding

This work was supported by the Russian Science Foundation (grant no. 21-75-20145).

Declaration of competing interest

The authors declare that they have no known competing financial interests or personal relationships that could have appeared to influence the work reported in this paper.

Acknowledgments

We would like to thank Alina G. Mikhailova for reviewing the paper and our collaborators from the Center for Mitochondrial Functional Genomics at Immanuel Kant Baltic Federal University and employees of the Department of Traumatology and Orthopedics of the Federal Center for High Medical Technologies, a Federal State Budgetary Institution of the Ministry of Health of the Russian Federation, for providing support. Fig. 3A–D, and E were created using Biorender.com.

Appendix A. Supplementary data

Supplementary data to this article can be found online at https://doi.org/10.1016/j.mitoco.2025.08.001.

References

1. Attardi G, Yoneda M, Chomyn A. Complementation and segregation behavior of disease-causing mitochondrial DNA mutations in cellular model systems. *Biochim Biophys Acta*. 1995;1271:241–248. https://doi.org/10.1016/0925-4439(95)00034-2.
2. Moraes CT, Schon EA. Detection and analysis of mitochondrial DNA and RNA in muscle by in situ hybridization and single-fiber PCR. *Methods Enzymol*. 1996;264:522–540. https://doi.org/10.1016/s0076-6879(96)64046-4.
3. He Y, Wu J, Dressman DC, et al. Heteroplasmic mitochondrial DNA mutations in normal and tumour cells. *Nature*. 2010;464:610–614. https://doi.org/10.1038/nature08802.
4. Li M, Schönberg A, Schaefer M, Schroeder R, Nasidze I, Stoneking M. Detecting heteroplasmy from high-throughput sequencing of complete human mitochondrial DNA genomes. *Am J Hum Genet*. 2010;87:237–249. https://doi.org/10.1016/j.ajhg.2010.07.014.
5. Li M, Schröder R, Ni S, Madea B, Stoneking M. Extensive tissue-related and allele-related mtDNA heteroplasmy suggests positive selection for somatic mutations. *Proc Natl Acad Sci U S A*. 2015;112:2491–2496. https://doi.org/10.1073/pnas.1419651112.
6. Michikawa Y, Mazzucchelli F, Bresolin N, Scarlato G, Attardi G. Aging-dependent large accumulation of point mutations in the human mtDNA control region for replication. *Science*. 1999;286:774–779. https://doi.org/10.1126/science.286.5440.774.
7. Harman D. The biologic clock: the mitochondria? *J Am Geriatr Soc*. 1972;20:145–147. https://doi.org/10.1111/j.1532-5415.1972.tb00787.x.
8. Beckman KB, Ames BN. The free radical theory of aging matures. *Physiol Rev*. 1998;78:547–581. https://doi.org/10.1152/physrev.1998.78.2.547.
9. Lee HC, Pang CY, Hsu HS, Wei YH. Differential accumulations of 4,977 bp deletion in mitochondrial DNA of various tissues in human ageing. *Biochim Biophys Acta*. 1994;1226:37–43. https://doi.org/10.1016/0925-4439(94)90056-6.
10. Lacan M, Thèves C, Keyser C, et al. Detection of age-related duplications in mtDNA from human muscles and bones. *Int J Leg Med*. 2011;125:293–300. https://doi.org/10.1007/s00414-010-0440-x.
11. Bruyère O, Honvo G, Veronese N, et al. An updated algorithm recommendation for the management of knee osteoarthritis from the european society for clinical and economic aspects of osteoporosis, osteoarthritis and musculoskeletal diseases (ESCEO). *Semin Arthritis Rheum*. 2019;49:337–350. https://doi.org/10.1016/j.semarthrit.2019.04.008.
12. Nekhaeva E, Bodyak ND, Kraytsberg Y, et al. Clonally expanded mtDNA point mutations are abundant in individual cells of human tissues. *Proc Natl Acad Sci U S A*. 2002;99:5521–5526. https://doi.org/10.1073/pnas.072670199.
13. Lacan M, Thèves C, Amory S, et al. Detection of the A189G mtDNA heteroplasmic mutation in relation to age in modern and ancient bones. *Int J Leg Med*. 2009;123:161–167. https://doi.org/10.1007/s00414-008-0266-y.
14. Thèves C, Keyser-Tracqui C, Crubézy E, Salles J-P, Ludes B, Telmon N. Detection and quantification of the age-related point mutation A189G in the human mitochondrial DNA. *J Forensic Sci*. 2006;51:865–873. https://doi.org/10.1111/j.1556-4029.2006.00163.x.
15. Wang Y, Michikawa Y, Mallidis C, et al. Muscle-specific mutations accumulate with aging in critical human mtDNA control sites for replication. *Proc Natl Acad Sci U S A*. 2001;98:4022–4027. https://doi.org/10.1073/pnas.061013598.
16. Samuels DC, Li C, Li B, et al. Recurrent tissue-specific mtDNA mutations are common in humans. *PLoS Genet*. 2013;9, e1003929. https://doi.org/10.1371/journal.pgen.1003929.
17. Arbeithuber B, Hester J, Cremona MA, et al. Age-related accumulation of de novo mitochondrial mutations in mammalian oocytes and somatic tissues. *PLoS Biol*. 2020;18, e3000745. https://doi.org/10.1371/journal.pbio.3000745.
18. Marita James. Isolation of high-quality, highly enriched mitochondrial DNA from mouse tissues v1. *Protocolsio*. 2018. https://doi.org/10.17504/protocols.io.mycc7sw.
19. Roy-Engel AM, Carroll ML, Vogel E, et al. Alu insertion polymorphisms for the study of human genomic diversity. *Genetics*. 2001;159:279–290. https://doi.org/10.1093/genetics/159.1.279.
20. Batzer MA, Deininger PL. Alu repeats and human genomic diversity. *Nat Rev Genet*. 2002;3:370–379. https://doi.org/10.1038/nrg798.
21. *Bbmap: A Fast, Accurate, Splice-Aware Aligner*. 2014.
22. Li H. Aligning sequence reads, clone sequences and assembly contigs with BWA-MEM. *arXiv [q-bioGN]*. 2013. https://doi.org/10.48550/ARXIV.1303.3997.
23. Battle SL, Puiu D, , TOPMed mtDNA Working Group, Verlouw J, Broer L, Boerwinkle E. A bioinformatics pipeline for estimating mitochondrial DNA copy number and heteroplasmy levels from whole genome sequencing data. *NAR Genom Bioinform*. 2022;4, lqac034. https://doi.org/10.1093/nargab/lqac034.
24. Khanna A, Larson DE, Srivatsan SN, et al. Bam-readcount - rapid generation of basepair-resolution sequence metrics. *ArXiv*. 2021;7:3722. https://doi.org/10.21105/joss.03722.
25. Laricchia KM, Lake NJ, Watts NA, et al. Mitochondrial DNA variation across 56,434 individuals in gnomAD. *Genome Res*. 2022;32:569–582. https://doi.org/10.1101/gr.276013.121.

26. Bolze A, Mendez F, White S, et al. A catalog of homoplasmic and heteroplasmic mitochondrial DNA variants in humans. https://doi.org/10.1101/798264; 2019.
27. Virtanen P, Gommers R, Oliphant TE, et al. SciPy 1.0: fundamental algorithms for scientific computing in python. *Nat Methods*. 2020;17:261–272. https://doi.org/10.1038/s41592-019-0686-2.
28. Vallat R. Pingouin: statistics in python. *J Open Source Softw*. 2018;3:1026. https://doi.org/10.21105/joss.01026.
29. Zuker M. Mfold web server for nucleic acid folding and hybridization prediction. *Nucleic Acids Res*. 2003;31:3406–3415. https://doi.org/10.1093/nar/gkg595.
30. Killilea DW, Killilea AN. Mineral requirements for mitochondrial function: a connection to redox balance and cellular differentiation. *Free Radic Biol Med*. 2022;182:182–191. https://doi.org/10.1016/j.freeradbiomed.2022.02.022.
31. Li J, Rohs R. Deep DNAshape webserver: prediction and real-time visualization of DNA shape considering extended k-mers. *Nucleic Acids Res*. 2024;52:W7–W12. https://doi.org/10.1093/nar/gkae433.
32. Li J, Chiu T-P, Rohs R. Predicting DNA structure using a deep learning method. *Nat Commun*. 2024;15:1–12. https://doi.org/10.1038/s41467-024-45191-5.
33. Liu Y, Zhang Z, Li T, Xu H, Zhang H. Senescence in osteoarthritis: from mechanism to potential treatment. *Arthritis Res Ther*. 2022;24:174. https://doi.org/10.1186/s13075-022-02859-x.
34. Whittaker JL, Losciale JM, Juhl CB, et al. Risk factors for knee osteoarthritis after traumatic knee injury: a systematic review and meta-analysis of randomised controlled trials and cohort studies for the OPTIKNEE consensus. *Br J Sports Med*. 2022;56:1406–1421. https://doi.org/10.1136/bjsports-2022-105496.
35. Yuan Y, Ju YS, Kim Y, et al. Comprehensive molecular characterization of mitochondrial genomes in human cancers. *Nat Genet*. 2020;52:342–352. https://doi.org/10.1038/s41588-019-0557-x.
36. Ludwig LS, Lareau CA, Ulirsch JC, et al. Lineage tracing in humans enabled by mitochondrial mutations and single-cell genomics. *Cell*. 2019;176, e22. https://doi.org/10.1016/j.cell.2019.01.022, 1325–39.
37. Tomasetti C, Vogelstein B. Cancer etiology. Variation in cancer risk among tissues can be explained by the number of stem cell divisions. *Science*. 2015;347:78–81. https://doi.org/10.1126/science.1260825.
38. da Costa CK, Kiyomoto BH, Schmidt B, Oliveira ASB, Gabbai AA, Tengan CH. Age-related mitochondrial DNA point mutations in patients with mitochondrial myopathy. *J Neurol Sci*. 2007;263:139–144. https://doi.org/10.1016/j.jns.2007.07.006.
39. Kashani K, Rosner MH, Ostermann M. Creatinine: from physiology to clinical application. *Eur J Intern Med*. 2020;72:9–14. https://doi.org/10.1016/j.ejim.2019.10.025.
40. Kashani K, Rosner MH, Ostermann M. Corrigendum to "creatinine: from physiology to clinical application"[European journal of internal medicine 72C (2020) 9-14]. *Eur J Intern Med*. 2023;116:168–169. https://doi.org/10.1016/j.ejim.2023.07.025.
41. Sullivan GM, Feinn R. Using effect Size-or why the P value is not enough. *J Grad Med Educ*. 2012;4:279–282. https://doi.org/10.4300/JGME-D-12-00156.1.
42. Tan BG, Mutti CD, Shi Y, et al. The human mitochondrial genome contains a second light strand promoter. *Mol Cell*. 2022;82, e9. https://doi.org/10.1016/j.molcel.2022.08.011, 3646–60.
43. Plaza-G AI, Lemishko KM, Crespo R, et al. Mechanism of strand displacement DNA synthesis by the coordinated activities of human mitochondrial DNA polymerase and SSB. *Nucleic Acids Res*. 2023;51:1750–1765. https://doi.org/10.1093/nar/gkad037.
44. Oguey C, Foloppe N, Hartmann B. Understanding the sequence-dependence of DNA groove dimensions: implications for DNA interactions. *PLoS One*. 2010;5, e15931. https://doi.org/10.1371/journal.pone.0015931.
45. Hillen HS, Morozov YI, Sarfallah A, Temiakov D, Cramer P. Structural basis of mitochondrial transcription initiation. *Cell*. 2017;171, e10. https://doi.org/10.1016/j.cell.2017.10.036, 1072–81.
46. Falkenberg M, Gustafsson CM. Mammalian mitochondrial DNA replication and mechanisms of deletion formation. *Crit Rev Biochem Mol Biol*. 2020;55:509–524. https://doi.org/10.1080/10409238.2020.1818684.
47. Sprason C, Tucker T, Clancy D. MtDNA deletions and aging. *Front Aging*. 2024;5, 1359638. https://doi.org/10.3389/fragi.2024.1359638.
48. Kraytsberg Y, Kudryavtseva E, McKee AC, Geula C, Kowall NW, Khrapko K. Mitochondrial DNA deletions are abundant and cause functional impairment in aged human substantia nigra neurons. *Nat Genet*. 2006;38:518–520. https://doi.org/10.1038/ng1778.
49. Gupta R, Kanai M, Durham TJ, et al. Nuclear genetic control of mtDNA copy number and heteroplasmy in humans. *Nature*. 2023;620:839–848. https://doi.org/10.1038/s41586-023-06426-5.
50. Wanrooij PH, Uhler JP, Simonsson T, Falkenberg M, Gustafsson CM. G-quadruplex structures in RNA stimulate mitochondrial transcription termination and primer formation. *Proc Natl Acad Sci U S A*. 2010;107:16072–16077. https://doi.org/10.1073/pnas.1006026107.
51. Agaronyan K, Morozov YI, Anikin M, Temiakov D. Mitochondrial biology. Replication-transcription switch in human mitochondria. *Science*. 2015;347:548–551. https://doi.org/10.1126/science.aaa0986.
52. Lott MT, Leipzig JN, Derbeneva O, et al. mtDNA variation and analysis using mitomap and mitomaster. *Curr Protoc Bioinformatics*. 2013;44. https://doi.org/10.1002/0471250953.bi0123s44, 1.23.1–26.
53. PhyloTree.org n.d. https://www.phylotree.org/tree/index.htm (accessed September 17, 2024).
54. Ghosh R, Hwang SM, Cui Z, Gilda JE, Gomes AV. Different effects of the nonsteroidal anti-inflammatory drugs meclofenamate sodium and naproxen sodium on proteasome activity in cardiac cells. *J Mol Cell Cardiol*. 2016;94:131–144. https://doi.org/10.1016/j.yjmcc.2016.03.016.
55. Mazumder S, De R, Sarkar S, et al. Selective scavenging of intra-mitochondrial superoxide corrects diclofenac-induced mitochondrial dysfunction and gastric injury: a novel gastroprotective mechanism independent of gastric acid suppression. *Biochem Pharmacol*. 2016;121:33–51. https://doi.org/10.1016/j.bcp.2016.09.027.
56. Boelsterli UA, Redinbo MR, Saitta KS. Multiple NSAID-Induced hits injure the small intestine: underlying mechanisms and novel strategies. *Toxicol Sci*. 2013;131:654–667. https://doi.org/10.1093/toxsci/kfs310.
57. Ralph SJ, Pritchard R, Rodríguez-Enríquez S, Moreno-Sánchez R, Ralph RK. Hitting the bull's-eye in metastatic Cancers-NSAIDs elevate ROS in mitochondria, inducing malignant cell death. *Pharmaceuticals*. 2015;8:62–106. https://doi.org/10.3390/ph8010062.
58. Lichtenberger LM, Zhou Y, Jayaraman V, et al. Insight into NSAID-induced membrane alterations, pathogenesis and therapeutics: characterization of interaction of NSAIDs with phosphatidylcholine. *Biochim Biophys Acta*. 2012;1821:994–1002. https://doi.org/10.1016/j.bbalip.2012.04.002.
59. Debsharma S, Pramanik S, Bindu S, et al. Honokiol, an inducer of sirtuin-3, protects against non-steroidal anti-inflammatory drug-induced gastric mucosal mitochondrial pathology, apoptosis and inflammatory tissue injury. *Br J Pharmacol*. 2023;180:2317–2340. https://doi.org/10.1111/bph.16070.
60. Debsharma S, Pramanik S, Bindu S, et al. NSAID targets SIRT3 to trigger mitochondrial dysfunction and gastric cancer cell death. *iScience*. 2024;27, 109384. https://doi.org/10.1016/j.isci.2024.109384.
61. Mazumder S, Bindu S, De R, Debsharma S, Pramanik S, Bandyopadhyay U. Emerging role of mitochondrial DAMPs, aberrant mitochondrial dynamics and anomalous mitophagy in gut mucosal pathogenesis. *Life Sci*. 2022;305, 120753. https://doi.org/10.1016/j.lfs.2022.120753.
62. Mazumder S, De R, Debsharma S, et al. Indomethacin impairs mitochondrial dynamics by activating the PKCζ-p38-DRP1 pathway and inducing apoptosis in gastric cancer and normal mucosal cells. *J Biol Chem*. 2019;294:8238–8258. https://doi.org/10.1074/jbc.RA118.004415.
63. Weinheimer EM, Jemiolo B, Carroll CC, et al. Resistance exercise and cyclooxygenase (COX) expression in human skeletal muscle: implications for COX-inhibiting drugs and protein synthesis. *Am J Physiol Regul Integr Comp Physiol*. 2007;292:R2241–R2248. https://doi.org/10.1152/ajpregu.00718.2006.
64. Damer A, El Meniawy S, McPherson R, Wells G, Harper M-E, Dent R. Association of muscle fiber type with measures of obesity: a systematic review. *Obes Rev*. 2022;23, e13444. https://doi.org/10.1111/obr.13444.